RELAXATIONAL DISLOCATION DAMPING DUE TO DISLOCATION-DISLOCATION INTERSECTIONS WITH APPLICATION TO MAGNESIUM SINGLE CRYSTALS

J. M. Roberts*

Rice University
Houston, Texas, U. S. A.

Paper to be presented at the International Conference on the Strength of Metals and Alloys, Tokyo, Japan, Sept. 4-8, 1967

* Dr. John M. Roberts, Associate Professor of Materials Science, William Marsh Rice University, Houston, Texas, U. S. A.

RELAXATIONAL DISLOCATION DAMPING DUE TO DISLOCATION-DISLOCATION INTERSECTIONS WITH APPLICATION TO MAGNESIUM SINGLE CRYSTALS

ABSTRACT

The preliminary results of an experimental investigation concerning the effect of temperature (in the range 82-320° K), frequency (in the range 0.015-0.75 cps) and stress amplitude (in the range 700-2700 gm/cm^2) upon the decrement in 99.96 atomic per cent magnesium single crystal, slightly prestrained, were reported by Roberts and Hartman[1]. Further experimental work concerning the modulus defect at almost zero stress for both 99.96 per cent pure magnesium crystals and crystals doped with small amounts of Al, Zn, Cd, Th and In has been carried out at 293° K. The results consistently show a static isothermal modulus defect of $\simeq$ 5% at almost zero stress even for impure crystals. This suggests that the dislocations are bowing between their nodal points from almost zero stress. As a result of this it is more likely a dislocation-dislocation intersection mechanism is the source of the damping and not a dislocation-solute atom interaction mechanism as previously reported by Roberts and Hartman[1]. A brief outline of Alefeld's theory[2] for relaxational, amplitude dependent dislocation damping due to dislocation intersections is presented. Details concerning how the previously cited experimental data can be treated to be applicable to this theory are presented.

---

[1] J. M. Roberts and D. E. Hartman: Phys. Soc. of Japan, 18, Supp. 1, (1963), 119.

[2] G. Alefeld: Zeitschrift für Physic, 170, (1962), 249.

The main features of all of the experimental results are semi-quantitatively explained by the superposition of several relaxation processes (28 in all) of the type proposed by Alefeld[2]. The activation energies of these processes vary between 0.34 to 0.98 ev. and the activation length of dislocation between approximately 1000 to 12,000 Burgers vector units. The strongest peaks have activation energies of 0.56, 0.65, 0.68, 0.75, 0.81 and 0.86 ev. with associated activation lengths of 910, 2730, 1820, 910, 606, and 910 Burgers vector units respectively. The microscopic work hardening coefficient acting upon dislocations has been evaluated and is in reasonable agreement with the experimentally observed damping loop. It is also compatible with a 5 to 10% modulus defect at almost zero stress. Qualitative arguments are suggested to justify the use of a spectrum of activation energies and dislocation loop lengths to explain amplitude dependent dislocation damping data. Particularly data taken at low frequencies when the single mechanism of dislocations cutting other dislocations via a thermally activated process is active.

INTRODUCTION

Birnbaum and Levy[3] were the first to predict that the thermally activated process of dislocations cutting other dislocations would lead to a measurable high temperature internal friction loss. They assumed that the source of energy dissipation would be due to the formation of jogs and point defects by the moving dislocation intersecting other dislocations. Their development appears weak, however, since they assumed

---

[3] H. Birnbaum and M. Levy: Acta. Met., 4, (1956), 84.

a Koehler distribution[4] for the loop lengths between jogs and that the rate of point defect production was proportional to the macroscopic strain rate. The first assumption presumes jogs are situated along the dislocation lines completely randomly, the reason for which is certainly not obvious. The second assumption does not contain the fact that the rate of point defect production should be proportional to the strain rate and possibly some function of the strain. Thus integration of the energy loss equation is required over both the loop length distribution and over time for one cycle. The latter was avoided in their original paper. Birnbaum and Levy found the log of the decrement to be proportional to T^{-1} and independent of frequency. These rather simple temperature and frequency dependences undoubtedly arise because of the weakness outlined above in their second assumption.

Certain phenomena related to internal friction such as stress relaxation at constant strain and strain relaxation at constant stress have been formalized by Zener[5], Kuhlmann-Wilsdorf[6], Seeger[7], Roberts and Brown[8] and more recently by Reed-Hill and Dahlberg[9] in which the dislocation-dislocation interaction mechanism at repulsive junctions is inferred

---

[4] J. S. Koehler: Imperfections in Nearly Perfect Crystals, John Wiley and Sons, (1952), 197.

[5] C. Zener: Cold Working of Metals, Amer. Soc. Metals, Cleveland, (1949), 180.

[6] D. Kuhlmann: Z. Phys. 124, (1947), 468.

[7] A. Seeger: Z. Naturf. 9a, (1954), 758.

[8] J. M. Roberts and N. Brown: Acta. Met., 11, (1963), 7.

[9] R. E. Reed-Hill and E. P. Dahlberg, Trans. A.I.M.E., 236, (1966), 679.

as the rate controlling mechanism. This group of authors, however, have not undertaken a rigorous application of this mechanism to internal friction.

The problem of a detailed formal derivation of the internal friction associated with dislocation-dislocation intersections at repulsive dislocation junctions was taken up by Alefeld[2]. It is the purpose of the present paper to put forth the main precedictions of Alefeld's theory and describe how we have applied this theory to our experimental results on magnesium single crystals.

SUMMARY OF ALEFELD'S THEORY

Consider a single thermally activated process for a dislocation intersecting a second repulsive dislocation. The overall strain rate, considering both forward and reverse jumps, is given by:

$$\dot{\epsilon}_a = 2b(\Delta A)N\nu_o \left\{\exp\left[\frac{\Delta S}{k}\right]\right\}\left\{\exp\left[\frac{-\Delta H}{kT}\right]\right\} \sinh\left\{\frac{(\sigma_a-\sigma_i)V}{kT}\right\} \quad (1)$$

where

ϵ_a is the plastic or anelastic shear strain,

b is the Burgers vector of the mobile dislocation,

ΔA is the area swept out by the mobile dislocation per intersection,

N is the number of intersection sites per unit volume,

ν_o is the dislocation attack frequency,

ΔS is the entropy change during the process,

ΔH is the enthalpy change during the process,

σ_a is the applied stress,

σ_i is the local resisting internal stress,

V is the activation volume given by ℓ b d,

ℓ is the average length of dislocation arc overcoming the barrier,

d is the activation distance, and

k and T have their usual meaning.

The first basic simplifying assumptions which will be made in using this equation are that V, hence ℓ and d, ΔA, N, ν_o and ΔS are taken to be independent of σ_a. Over a small strain increment σ_i is given by $\theta\epsilon_a$, where θ is the microscopic work hardening coefficient acting upon the mobile dislocations. Using $\sigma_a = \epsilon_e M_u$, where ϵ_e is the elastic strain and M_u is the unrelaxed shear modulus for the material in question and $\Delta_m = M_u/\theta$ it is readily shown:

$$\dot{\epsilon}_a = -\frac{1}{\tau}\left\{\epsilon_a - \Delta_m \epsilon_e\right\} \tag{2}$$

where the relaxation time τ is given by:

$$\tau = \frac{\left\{\frac{kT}{V\theta}\right\} \exp\left\{\frac{\Delta H}{kT}\right\}}{2b(\Delta A)N\left\{\exp\left[\frac{\Delta S}{k}\right]\right\}\nu_o} \quad . \tag{3}$$

The total strain, ϵ, is given by $\epsilon_a + \epsilon_e$. The governing differential equation for the deformation of the body neglecting any specific damping due to the dislocation velocity is:

$$\ddot{\epsilon} + \omega^2 \epsilon_e = 0 \tag{4}$$

where $\omega = 2\pi\nu$ and ν is the frequency of a stress cycle. In general the

total strain is given by:

$$\epsilon = a \sin (\omega t + \varphi) \tag{5}$$

where a is the strain amplitude and φ is the phase angle between the strain in phase and out of phase with the applied stress. Application of the formal theory for free and forced vibrations of a damped linear oscillator yields:

$$a = a_o \left\{ \exp \left[- \frac{\Delta \omega t}{2\pi} \right] \right\} \tag{6}$$

where Δ, the logarithmic decrement, is given by:

$$\Delta = - \frac{2\dot{a}}{\omega a} \tag{7}$$

and a_o is the maximum strain amplitude. One also obtains

$$\delta = \frac{\Delta M}{M} = \frac{M_u - M_R}{M_u} = - \frac{2\dot{\varphi}}{\omega} \tag{8}$$

where M_R is the completely relaxed modulus. The development demands Δ and $\Delta M/M$ are < 1 .

Substitution of equation (5) into equation (4), and solving for ϵ_a, then carrying out an integration over $(\omega t + \varphi)$ from 0 to 2π and integrating by parts once, it may be shown that:

$$\Delta = \frac{\Delta_m \left\{ \frac{\omega\tau}{f(z)} \right\}}{\left[1 + \left(\frac{\omega\tau}{f(z)} \right)^2 \right]} \tag{9}$$

and

$$\delta = \frac{\Delta_m}{\left[1 + \left(\frac{\omega\tau}{f(z)} \right)^2 \right]} \tag{10}$$

where $f(z) = \frac{2I_1(z)}{(z)}$ and $I_1(z)$ is the modified Bessel function of the first kind. In equations (9) and (10), z is given by:

$$z = \frac{VM_u a}{kT}\left(1 + \left\{\frac{f(z)}{\omega\tau}\right\}^2\right)^{-\frac{1}{2}} \quad . \tag{11}$$

For $z < 1$, $f(z)$ may be expanded as

$$f(z) = 1 + \frac{z^2}{8} + \frac{z^4}{192} + z^6\left(\frac{1}{2}\right)^7\left(\frac{1}{3!}\right)\left(\frac{1}{4!}\right) + + \tag{12}$$

and for $z > 8$, $f(z)$ is accurately described by:

$$f(z) = \left(\frac{2}{\pi}\right)^{\frac{1}{2}} z^{-\frac{3}{2}} e^z \quad . \tag{13}$$

Alefeld[7] has made a plot of $f(z)$ versus z for z in the range 1 to 100. For a given V, M_u, a, T, ω and τ there will only be one z and $f(z)$ that will satisfy equation (11). The value of $f(z)$, may then be placed in equations (9) and (10) along with the prescribed values of ω, τ, M_u and θ and hence Δ and δ may be evaluated.

APPLICATION OF ALEFELD'S THEORY TO EXPERIMENT

The unidirectional damping loops observed by Roberts and Hartman[1] for magnesium single crystals are believed to be good examples of internal friction experimental data to which Alefeld's theory is applicable. If the damping loops can be explained upon the basis of dislocations cutting forest dislocations even at vanishingly low stress, then at almost zero stress the dislocation lines should not be pinned by impurities. This is expected to be the case at very low frequencies, which is the situation in

these experiments. Table I shows values of the isothermal Young's modulus (E_s) for various purity magnesium single crystals. The measured values are shown in one column and the values calculated from the known orientation of each crystal and the published adiabatic elastic constants of magnesium in another. A modulus defect of about 10% at almost zero stress is consistently observed for high purity magnesium crystals. It is important to note that significant amounts of substitutional solute atoms (Al, Zn, Cd, In or Th) in the magnesium does not alter the fact that a modulus defect of about 5% is observed at almost zero stress.

Consider that a random three-dimensional Frank network of dislocations exist in these crystals of average length ℓ between nodal points. If a certain fraction, α, of the network bows out at almost zero stress, a modulus defect[10] given by:

$$-\frac{\delta E}{E} = -\frac{\delta M}{M} \backsim 0.72\ \alpha\ N\ \ell^3 \qquad (14)$$

where N is the number of loops per unit volume is expected. Since $3N\ell^3 \backsim 1$ and $\alpha \backsim \frac{1}{3}$, $-\frac{\delta E}{E} \backsim 0.08$ which is in reasonable agreement with the modulus defects shown in Table I. This observation makes the dislocation-dislocation intersection mechanism a strong contender, if not the only one, to explain the observed internal friction results.

insert Figure 1 ←

Figure 1 shows a schematic diagram of a typical unidirectional damping loop ie. (1-2-3-4-1). The ordinate is the applied stress, σ_a, and the abscissa is the total strain, a, in phase with σ_a. In this figure a_o would be the maximum strain amplitude for this loop. The area (1-2-3-4-1)

---

[10] J. Friedel: Dislocations, Addison-Wesley, (1964), 235 and 61.

TABLE I

METAL	CRYSTAL	E_s (calculated) (gm/mm^2) $\times 10^6$	E_s (measured) (gm/mm^2) $\times 10^6$	Modulus Defect (%)	REF.
99.95 weight % Mg.	MS-2	9.12	8.44	7.5	1
99.95 weight % Mg.	MS-3	8.90	8.25	7.2	1
99.95 weight % Mg.	MS-4	9.16	8.17	7.8	1
99.95 weight % Mg.	MS-5	9.33	8.10	13.1	1
99.95 weight % Mg.	MS-6	9.01	8.94	16.6	1
99.95 weight % Mg plus 0.048 atomic % Al	3A1A	4.43	4.19	5.4	11
99.95 weight % Mg plus 0.460 atomic % Al	5A1	4.51	4.44	1.6	11
99.95 weight % Mg plus 0.168 atomic % Zn	4Z4	4.42	4.23	4.3	11
99.95 weight % Mg plus 0.090 atomic % Cd	4C8	4.41	4.30	2.5	11
99.95 weight % Mg plus 0.045 atomic % Th	4T1	4.41	3.69	16.3	11
99.95 weight % Mg plus 0.165 atomic % In	4I2	4.41	4.26	3.4	11

[11] D. E. Hartman: Ph.D. Thesis, W. M. Rice University, Houston, Texas, May, (1965).

is W_{irr}, the energy loss, and the area (1-2-3-5-1) is W_T, hence Δ is the ratio of the two areas.

We now need some way to evaluate a reasonable value of θ (the microscopic work hardening coefficient). From the work of Hartman[12] on magnesium single crystals, it was found empirically for the loading portion of the loop that:

$$\sigma_a = Ca^p \tag{15}$$

where $C = 7.04 \times 10^6$ gm/cm^2 and $p = 3/4$. This empirical relation holds up fairly well in the temperature region 82° K to 320° K and the frequency range 0.015 to 0.75 cps. Equation (15) may be written in the form

$$\left(\frac{\sigma_a}{C}\right)^{1/p} = a_e + a_a \tag{16}$$

where a_e is the elastic strain in phase with σ_a, and a_a is the anelastic strain in phase with σ_a. The microscopic work hardening coefficient θ is then $\frac{d\sigma_a}{da_a}$ and noting $\frac{da_e}{da_a} = \frac{\theta}{M_u}$, θ is evaluated as

$$\theta = \frac{pCa^{p-1}}{1 - \frac{1}{M_u} pCa^{p-1}} \tag{17}$$

Since the mean amplitude of most of the damping loops (a_m, Figure 1) is $\sim 2 \times 10^{-5}$, equation (17) has been expanded in a Taylor series about a_m to yield:

$$\theta = 1.45 \times 10^8 - (7.23 \times 10^{11})(a - 2.18 \times 10^{-5}) \tag{18}$$

---

[12] D. E. Hartman, M. Sc. Thesis, W. M. Rice University, Houston, Texas, May, (1961).

where θ is in gm/cm^2. M_u for magnesium is 1.69×10^8 gm/cm^2, so that equation (18) yields a modulus defect of 5% at a = 0 which agrees fairly well with experiment (Table 1). It should be pointed out that the amplitude dependence of the decrement, Δ equation (9), is primarily determined by the amplitude dependence of θ in Δ_m which equals $\frac{M_u}{\theta}$. Equation (18) for θ produces a slightly milder amplitude dependence for Δ than θ according to equation (17). This milder dependence had to be made to yield reasonable agreement between theory and experiment.

For any stress, σ_a, a is determined from equation (15) and θ from equation (18). Since $\omega = 2\pi\nu$ where ν is the reciprocal of the time to make a damping loop, ω is determined by experiment. σ_a and T are also determined by experiment and M_u and k are published constants. To complete the analysis for a single relaxation peak, one must evaluate τ (equation (3)). In order to reduce this problem to the two most important fundamental variables, ΔH and V, we have made the following approximations: $V = b^2\ell$, $\Delta A = \ell^2$, $N = \ell^{-3}$, $\nu_o = \nu_D \frac{b}{\ell}$ and $e^{\Delta S/k} = 10$ where ν_D is the atomic frequency $\underset{\sim}{\sim} 10^{13}$ sec^{-1} and all other terms have been previously defined. The above approximations mean the stress dependence of ℓ, d, ν_o and $\Delta S/k$ are being ignored. These approximations are not considered too serious for application to the dislocation intersection mechanism in magnesium crystals. Certainly the assumed stress independence of ℓ is the most serious. In any event, if one is to consider the stress dependence of ℓ or any other parameters, then Alefeld's theory would have to be markedly modified, a task which may or may not lead to a closed form solution.

For any given ΔH, and V, τ is evaluated from equation (3) and the solution of equation (11) for the appropriate values of z and f(z)

is obtained from the experimental conditions σ_a, T, and ν. This value of f(z) is then used to solve equation (9) for the logarithmic decrement (Δ). Such calculations have been carried out for ΔH in the range (0.10 to 3.0) ev. in steps of 0.1 ev., σ_a in the range (1 to 6000) gms/cm^2, T in the range (70 to 325)°K and V in the range (1×10^{-22} to 1×10^{-16}) cm^3 in decade steps.

The work by Saada[13] shows that the activation energy, at constant applied stress, to overcome a repulsive dislocation junction is dependent upon the relative orientation of the tangent and Burgers vectors of the two intersecting dislocations. There is certainly to be expected some variation in this relative orientation between different mobile and forest dislocations in a crystal. This means there must exist some spectrum of values for ΔH in equation (4). Also, the actual free length of mobile dislocation (ℓ) cutting a forest dislocation is not expected always to have one finite value. Therefore, we must really consider the possibility of some spectrum of values of ΔH and ℓ contributing to the overall observed damping phenomena. In such a case (at one frequency), equation (9) should be replaced by

$$\Delta_{calc} = \sum_{i=1}^{i=n} \frac{f_i (\Delta_m)_i \left\{ \frac{\omega\tau_i}{(f(z)_i} \right\}}{\left[1 + \left\{ \frac{\omega\tau_i}{f(z)_i} \right\}^2 \right]} \qquad (19)$$

where each subscript i refers to a particular set of ΔH_i and V_i (hence ℓ_i), Δ_{calc} is the predicted value of the observed decrement and f_i is a weighing

---

[13] V. G. Saada: Thèses présentées a la Faculté des Sciences de l'Université de Paris, (1960).

factor related to the fraction of the entire mobile dislocation network which is represented by particular values of ΔH_i, V_i and θ_i. By this definition, $\sum_{i=1}^{i=n} f_i$ should equal unity. The upper limit, n, of the summation is representative of the total number of processes, each of the dislocation-dislocation interaction type at repulsive junctions, contributing to the overall observed damping.

It is conceivable, over a small strain increment as in an internal friction measurement, that some of the dislocations may experience microscopic work hardening and others not. An attempt to take care of this possibility is included in the definition of θ_i in $(\Delta_m)_i$ and τ_i in equation (19). If the process exhibits work hardening (ie. θ_i is a function of the amplitude), then θ_i is given by equation (18) and will be designated $(\theta_i)_a$, if no microscopic work hardening is assumed θ_i is given by the value 1.61×10^8 gm/cm^2, representing a modulus defect of 4.7% at almost zero stress and will be designated as $(\theta_i)_N$.

insert FIGURE 2 ←

Figure 2 shows a plot of the observed decrement, Δ_{obs}, versus temperature for a high purity magnesium crystal after Roberts and Hartman[1]. Data points are shown for six different applied stress levels, the frequency, 0.0746 cps, was constant throughout. The significant features of these curves are:

(1) the peak at 270° K appears to be relatively independent of stress amplitude

(2) the broad peak at $\sim$ 230° K (σ_a = 1790 gm/cm^2) appears to increase with strain amplitude and shift to lower temperatures as the amplitude is increased

(3) the decrement on the low temperature side of the broad

peak appears to uniformly increase at constant temperature with increasing amplitude.

insert FIGURE 3 ←

Figure 3 shows a plot of the observed decrement versus temperature for a high purity magnesium crystal at six different frequencies all at one stress amplitude 1197 gm/cm^2. This data, hitherto unpublished, was determined in exactly the same manner as previously described by Roberts and Hartman[1]. A similar plot, only at a stress amplitude of 738 gm/cm^2 for the same crystal is published as Fig. 6 of the paper by Roberts and Hartman[1], and need not be reproduced here. The significant features of both Fig. 3 of this communication and Fig. 6 of the paper by Roberts and Hartman[1] are:

(1) The broad relaxation peak around 200° K at the lowest frequency, increases in temperature with increasing frequency as expected for a relaxation process, the apparent activation being $\underset{\sim}{\sim}$ 0.52 ev. for the data shown in Fig. 3 and $\underset{\sim}{\sim}$ 0.66 ev. for the previously published data by Roberts and Hartman[1].

(2) The maximum value of the decrement rises with increasing frequency at constant stress amplitude for both the data shown in Fig. 3 as well as that of Fig. 6 in the Roberts and Hartman paper.

Although many tests have been made of a similar nature to those shown in Figs. 2 and 3, it is impossible to publish all of the data. The data shown in Figs. 2 and 3 is representative of all other data runs, but in all honesty it is by far the most carefully taken and accurate data

available at this time. It was therefore considered worthwhile to investigate what sort of a spectrum for ΔH_i and ℓ_i in equation (19) is required to reasonably explain the features of these figures. An extensive computer program was set up to investigate all the ranges and combinations of ΔH, σ_a, T, and V previously described in this paper. To try and fit equation (19) to the previously described data, at first three or four processes were attempted. After an exhaustive search, with a gradually increasing number of processes, a reasonable correlation between theory and experiment was found with twenty-eight processes.

insert FIGURE 4 FIGURE 5 and FIGURE 6

Figure 4 shows a plot of Δ_{obs} versus temperature at one frequency and four stresses, superimposed upon Δ calculated (Δ_{calc}) from equation (19) for the 28 processes at the same frequency and stresses. Comparison of Figures 2 and 4, shows that the salient features of Fig. 2 (previously discussed) are explained by the superposition of twenty-eight processes. Figure 5 shows Δ_{calc} and Δ_{obs} versus temperature for one stress level and frequency as well as the twenty-eight individual processes. Figure 6 is a similar plot to Fig. 5 at the same frequency, yet at a different stress level. Comparison of Figs. 5 and 6 allows one to see how individual relaxation peaks are affected by a change in stress amplitude or activation volume. Table II lists the values of ΔH_i, $\frac{\ell_i}{b}$, f_i and θ_i (ie. if it is $(\theta_i)_a$ or $(\theta_i)_N$) for the twenty-eight processes which yield the results shown in Figs. 4, 5 and 6. For simplicity if θ_i is $(\theta_i)_a$ it is designated by A, and if θ_i is $(\theta_i)_N$ it is designated by B.

Some of the individual peaks in Table II are labeled on Figs. 5 and 6. A study of these figures shows:

(1) An increase in stress amplitude shifts a peak to lower

TABLE II

PROCESS	(ΔH_i)ev.	(ℓ_i/b)	$f_i \times 10^2$	θ_i	$\omega(1197)$	$\omega(738)$
1	0.34	910	1.37	A	$f_i = 1.14$	$f_i = 1.15$
2	0.40	910	2.73	A	$f_i = 4.75$	$f_i = 3.44$
3	0.42	910	3.64	A	$f_i = 5.81$	$f_i = 4.33$
4	0.46	910	2.34	A	$f_i = 3.85$ $\Delta H_i = 0.45$	$f_i = 3.87$ $\Delta H_i = 0.45$
5	0.47	910	3.45	A	$f_i = 5.75$	$f_i = 5.19$
6	0.50	910	3.45	A	$f_i = 4.14$	$f_i = 4.16$
7	0.52	910	3.36	A	$f_i = 4.48$	$f_i = 4.23$
8	0.56	910	4.52	A	$f_i = 6.35$	$f_i = 6.11$
9	0.61	910	3.12	B	$f_i = 4.20$	$f_i = 5.85$
10	0.62	6060	2.34	A	$f_i = 1.37$	$f_i = 1.96$
11	0.63	910	1.49	B	$f_i = 1.95$ $\Delta H_i = 0.62$	$f_i = 1.90$ $\Delta H_i = 0.62$
12	0.65	2730	4.68	A	$f_i = 3.90$	$f_i = 5.24$
13	0.68	910	1.09	B	$f_i = 2.18$ $\theta_i = A$	$f_i = 1.72$ $\Delta H_i = 0.070$ $\theta_i = A$
14	0.68	1820	4.68	B	$f_i = 0.00$	$f_i = 0.00$
15	0.70	910	2.98	B	$f_i = 2.87$ $\Delta H_i = 0.71$	$f_i = 2.39$ $\Delta H_i = 0.71$
16	0.73	910	2.73	B	$f_i = 2.27$	$f_i = 2.29$
17	0.75	910	4.62	A	$f_i = 3.85$	$f_i = 3.16$
18	0.76	2730	2.73	A	$f_i = 1.71$	$f_i = 1.72$
19	0.79	910	2.52	B	$f_i = 1.95$	$f_i = 1.96$
20	0.80	12,120	2.05	B	$f_i = 1.71$	$f_i = 1.72$
21	0.81	606	5.70	B	$f_i = 2.79$ $\ell_i/b = 910$	$f_i = 2.86$ $\ell_i/b = 910$
22	0.82	910	2.98	B	$f_i = 3.03$ $\Delta H_i = 0.83$	$f_i = 3.06$ $\Delta H_i = 0.83$
23	0.86	910	4.68	B	$f_i = 3.41$	$f_i = 3.44$
24	0.88	910	1.09	B	$f_i = 0.91$	$f_i = 0.92$
25	0.90	303	3.28	B	$f_i = 2.94$ $\ell_i/b = 910$	$f_i = 2.96$ $\ell_i/b = 910$
26	0.91	910	4.68	B	$f_i = 1.95$	$f_i = 1.96$
27	0.94	910	5.96	B	$f_i = 4.96$	$f_i = 5.00$
28	0.98	910	11.71	B	$f_i = 10.10$	$f_i = 10.20$

temperature (eg. peak 12).

(2) For the same or almost the same ΔH_i, an increase in ℓ_i/b caused the peak to become broader and shift to lower temperature (eg. compare peaks 20 and 21, or 17 and 18).

(3) When θ_i is $(\theta_i)_a$, the maximum value of the decrement increases with stress amplitude (eg. peaks 12, 17 and 18), whereas when θ_i is $(\theta_i)_N$, no change in the maximum values occurs with increasing amplitude, only the peak temperature changes.

To obtain a reasonable fit of equation (19) to the frequency data shown in Fig. 3 of this paper and Fig. 6 of the paper by Roberts and Hartman[1], minor changes had to be made to ΔH_i and $\frac{\ell_i}{b}$ for some of the 28 processes described in Table II. In addition, two new peaks needed to be added, one having characteristic values of $\Delta H_i = 0.55$ ev., $\ell_i/b = 910$, $f_i = 2.73 \times 10^{-2}$ and $\theta_i = A$ and the other $\Delta H_i = 0.65$ ev., $\ell_i/b = 910$, $f_i = 2.95 \times 10^{-2}$ and $\theta_i = B$ at the stress level 1197 gm/cm^2. At the stress level 738 gm/cm^2, f_i for these peaks are 3.98×10^{-2} and 3.73×10^{-2} respectively, all other values are the same. The column (ω 1197) in Table II shows the values of ΔH_i, ℓ_i/b, f_i and θ_i needed to obtain fair correlation between data and predictions for the variable frequency data at 1197 gm/cm^2. The column (ω 738) shows the same information as stated above for the variable frequency data taken at 738 gm/cm^2. In the columns (ω 1197) or (ω 738), only new values of f_i, θ_i, ΔH_i, or ℓ_i/b are shown. This means the values of ΔH_i, ℓ_i/b and θ_i are the same as those for the numbered process to the left if no new number is shown. In these two columns, it is assumed ΔH_i

is reported in electron volts, and f_i values should be multiplied by 10^{-2}.

Since the frequency effect data was measured on a different crystal (crystal MS-6) than the stress amplitude effect data (crystal MS-3), it is not unreasonable to assume a slightly different dislocation structure (hence ΔH_i, ℓ_i/b and f_i values) existed between the two specimens. A significant point, however, is that 29 processes, with almost the same values of ΔH_i and ℓ_i/b obtained to fit the stress amplitude data on crystal MS-3 can give reasonably good correlation with the variable frequency data on a different specimen (crystal MS-6). Figure 7 shows Δ_{obs} and Δ_{calc} versus temperature at σ_a = 738 gm/cm^2 for the lowest, highest and an intermediate frequency. Figure 8 is similar to that of Fig. 7, except data and correlation at σ_a = 1197 gm/cm^2 is shown. The individual 29 processes are also shown in these figures at the intermediate frequency to show their nature at a relatively low stress. Note that the calculated broad peak around 200° K (Fig. 8) or 225° K (Fig. 7) shifts to higher temperature with increasing frequency consistent with the observed peak shift data. Also, the maximum value of the calculated decrement rises with increasing frequency at constant stress, an unexpected feature which also agrees with the experimental data. Comparison of the numbered peaks in Figs. 5, 6, 7 and 8 shows clearly how rapidly the temperature at the peak maximum shifts upwards with decreasing stress amplitude.

It is unfortunate that slightly different values of f_i were required to fit the frequency data at the two stresses 1197 and 738 gm/cm^2, since the data was taken on the same crystal. This might reflect a mild stress amplitude dependence upon the mobile dislocation density. It is not possible at this time to incorporate such a dependency into the formal theory.

A study of Figs. 5-8, shows that at any one temperature, there are usually 4 to 7 processes active. One further calculation was made to test the internal consistency of this analysis. The observed strain rate in the damping loop region is $\gtrsim 10^{-8}$ to 10^{-5} sec^{-1} from the work of Roberts and Hartman[14]. For the ith process, the strain rate is given by $(\dot{\epsilon}_a)_i = f_i \dot{\epsilon}_a$ (equation (1)), where σ_i is given by $\theta_i f_i \epsilon_a$ and ϵ_a is approximately given by a_a in equation (16), when a_e is replaced by $(\frac{\sigma_a}{M_u})$. Using the values of all the parameters in equation (1) for each of the 28 processes described in Table II, $(\dot{\epsilon}_a)_i$ at each temperature was evaluated. When the process was operative $(\dot{\epsilon}_a)_i$ was found to have values between 10^{-5} to 10^{-9} sec^{-1}. If the temperature was well above the peak temperature, then $(\dot{\epsilon}_a)_i$ was very large which meant this process is completely relaxed and contributes to the overall strain but not the observed strain rate. At temperatures well below the peak temperature $(\dot{\epsilon}_a)_i$ was very small $\gtrsim 10^{-12}$ sec^{-1} or less, contributing negligibly to the observed strain rate. Therefore, it is encouraging that the strain rates calculated by this crude method for each active process at each temperature are of the same order of magnitude as the observed strain rate.

---

[14] J. M. Roberts and D. E. Hartman: Trans. A.I.M.E., 230, (1964), 1125.

DISCUSSION

We must clarify exactly what is meant by a spectrum of activation energies associated with the mechanism of dislocations cutting other dislocations at repulsive type junctions. There are two ways which this author can envisage as reasonable possibilities. The first way is to consider the elastic interaction potential as too large, so that ΔH is made up solely of the energy to form jogs or kinks, in extended or unextended dislocations, and or some point defects with or without their subsequent migration. To carry out such detailed atomic calculations near the vicinity of dislocation cores is a large undertaking, let alone taking into consideration a range of values for the tangent and Burgers vectors of the two interacting dislocations. Such calculations may lead to a spectrum of activation energies, so that this possibility cannot be outrightly discarded. There is, however, a simplier explanation and this is the one favored by this author.

insert Figure 9 ←

Figure 9(a), after the work of Saada[13], shows schematically the variation of the stress exerted between a repulsive dislocation upon a mobile dislocation as a function of distance. Figure 9(b) shows the variation of the stress exerted by special attractive dislocation upon a mobile dislocation. These particular attractive junctions must break down by the two triple nodes continuously moving together to form a quadruple node as the stress is increased. The peaks, (C), in these figures represent the jog formation process at the moment of complete cutting of one dislocation by the other. Depending upon the relative orientation of the tangent and Burgers vectors of the two intersecting dislocations these σ versus d curves, although having similar forms, can vary in scale. Figure 9(a) shows

two repulsive type junctions and Fig. 9(b) shows two special attractive type junctions each of varying scales as examples. There is in a real crystal, probably a spectrum of these types of σ-d relations. Saada[13] has shown that the activation energy necessary to surmount the elastic interaction potential (ie.) σ from 0.97 σ_M to σ_M(Fig. 9(b)) is $\underset{\sim}{\sim}$ 0.01 (ℓ/b) ev. or σ from 0.90 σ_M to σ_M(Fig. 9(a)) is $\underset{\sim}{\sim}$ 0.005 (ℓ/b) ev. for magnesium. For values of (ℓ/b) > 1000, these energies are large and could not be overcome by thermal agitation at low temperatures. This is precisely the reason why most investigators consider that the applied stress and local internal stresses must yield an effective stress equivalent to about σ_M for thermally activated flow controlled by dislocation intersections.

Since other dislocations than the two under consideration can provide a fluctuating internal stress σ_i throughout the crystal, it is possible at $\sigma_a = 0$, that for many junctions σ_i locally is as depicted in Fig. 9. The value of ΔH at $\sigma_a = 0$ is then represented by the hatched area in Fig. 9. σ_a would add on to σ_i and reduce the activation energy. Since there can be a spectrum of values of σ_i, and there exists a spectrum of figures of the type shown in Fig. 9 in a real crystal, there can exist a spectrum of values for ΔH. Of course, the particular set of conditions of σ_i and barrier scale would still require σ_i/σ_M to be close to 1 (eg. 0.9 to 0.999) for realistic values of (ℓ/b). This means, it is suggested the elastic interaction potential energy can contribute a small amount to the activation energy necessary to form a jog pair or the like near the intersection point and hence contribute to a spectrum of values of ΔH.

There is little doubt that both of the ways described in this paper actually contribute to a range of values for ΔH. It has only been the purpose in this discussion to justify the use of a number of different values

of ΔH_i in equation (19) to explain the data for magnesium, bearing in mind a single mechanism is still held as controlling the observed damping.

The energy necessary to form a jog in magnesium is $\sim \frac{M_u b^3}{10}$ (10) or $\sim$ 0.35 ev. The activation energy to form a pair of jogs is therefore $\sim$ 0.70 ev. which is in the middle of the ΔH_i values shown in Table II. This means that the local internal stress and σ_a act to place the effective stress just as often slightly above σ_M (Fig. 9) as slightly below this value. It is certainly encouraging that the determined values of ΔH_i are at least compatible with the order of magnitude estimate for the jog pair formation mechanism, the basic mechanism assumed to be operative in this paper. It is possible that some other mechanism could be conceived which would be compatible with this formal analysis. This author has not been able to find one which is as entirely consistent with this treatment as the dislocation intersection mechanism affords.

insert FIGURE 10 ←

Figure 10 shows a three-dimensional plot of f_i, ΔH_i and ℓ_i/b for the 28 processes which fit the variable stress amplitude data shown in Figs. 4, 5, and 6. The first rather surprising result is the large number of processes which have a somewhat small activation length of $\sim$ 1000 b, yet seem to have an erratic variation in weighing factors for different values of ΔH_i. A significant feature of the plot is that if one joins points a, b, c, d, e, and f, which have activation energies between 0.60 ev. and 0.82 ev., the weighing factors for loop lengths resemble in a small way a Koehler[4] type distribution. There is little doubt that if one wished to choose many more processes than 28, and decreased the weighing factors of all processes proportional to the number of multiples of 28 processes one selected, then a rather continuous distribution for ΔH_i, ℓ_i/b and f_i in the

ranges shown in Fig. 10 could be found. This quasi-continuous distribution would probably be able to fit all of the data just as well if not better than has been accomplished in this paper. Although, there have been found a rather large number of processes of somewhat small loop lengths ($\ell_i \gtrsim 1000$ b), these values are not unreasonable for the dislocation intersection mechanism. Vacancy or interstitial forming jogs may act as strong pins for some of the dislocations in the network.

There certainly could be other sets of values of ΔH_i, ℓ_i and f_i found which could probably explain the experimental results just as well as the set proposed here. One would find, however, that numerous processes are required and that only mild variations in these values could be tolerated. For example, if one wishes to use larger activation lengths, then as Figs. 5, 6, 7 and 8 show, these type of peaks are broad and shift in temperature rapidly with changing stress amplitude. Therefore, one would have a difficult time explaining the general features of the data in Figs. 2 and 3.

In summary we have found for low frequency high amplitude internal friction in magnesium, the obseved modulus defect at almost zero stress is explained by all the dislocation loops bowing between network nodal points and or point defect producing dislocation jogs and not between solute atom or point defect pins. That a spectrum of activation energies and activation loop lengths associated with the basic mechanism of dislocations intersecting other dislocations at primarily repulsive type junctions can explain rather consistently the main features of the damping loops observed in slightly prestrained magnesium single crystals.

ACKNOWLEDGMENTS

The author expresses his appreciation to Dr. D. E. Hartman for experimental assistance and Mr. Bill Mattair for his extensive assistance on an IBM 7040 Computer. The financial support of the National Aeronautics and Space Administration (Grant NsG-6-59) is gratefully acknowledged.

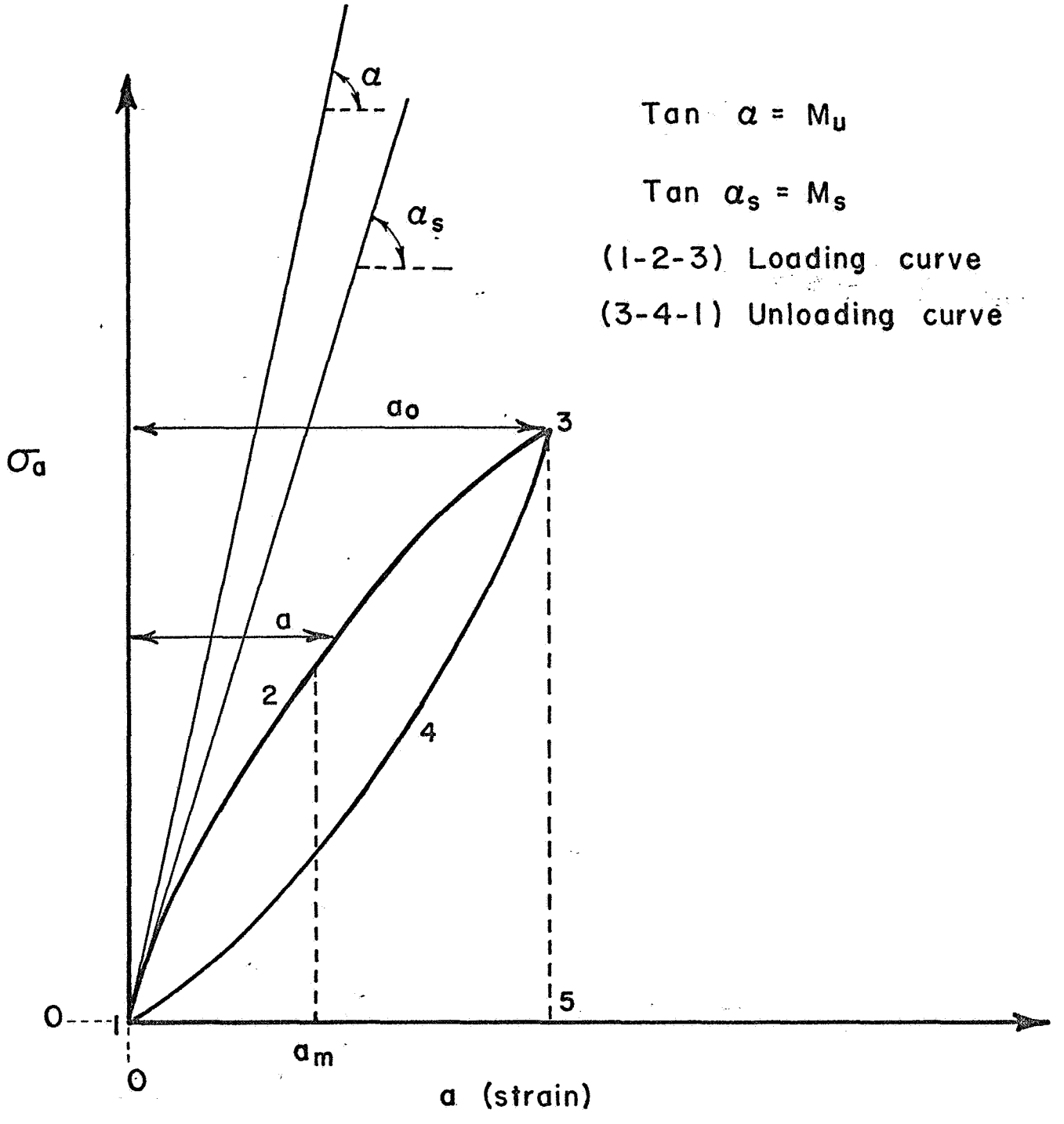

FIGURE 1: Schematic σ_a versus amplitude (a) plot to show features of a damping loop.

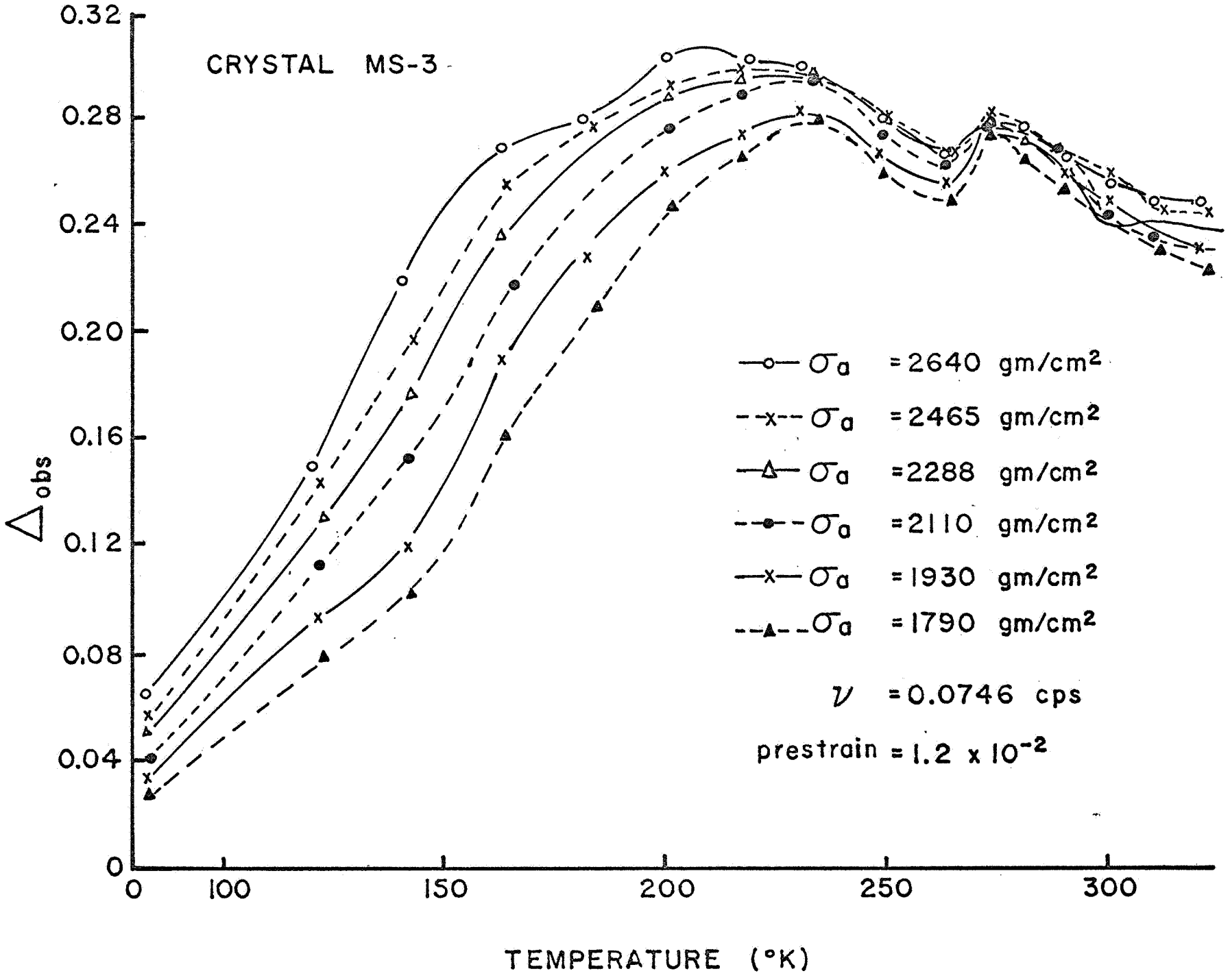

FIGURE 2: Δ_{obs} versus T at six stresses for crystal MS-3.

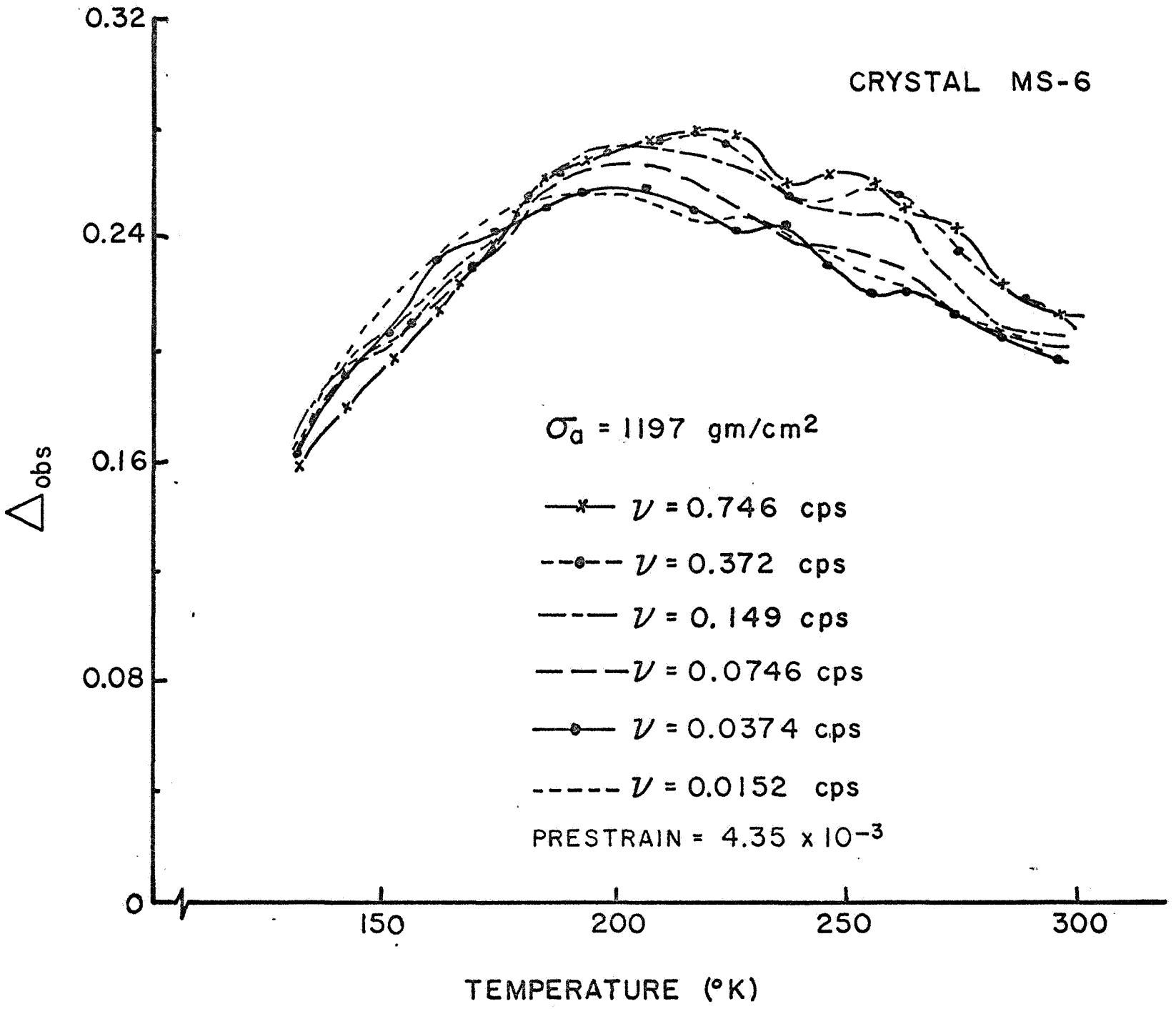

FIGURE 3: Δ_{obs} versus T at six frequencies and one stress (1197 gm/cm^2) for crystal MS-6.

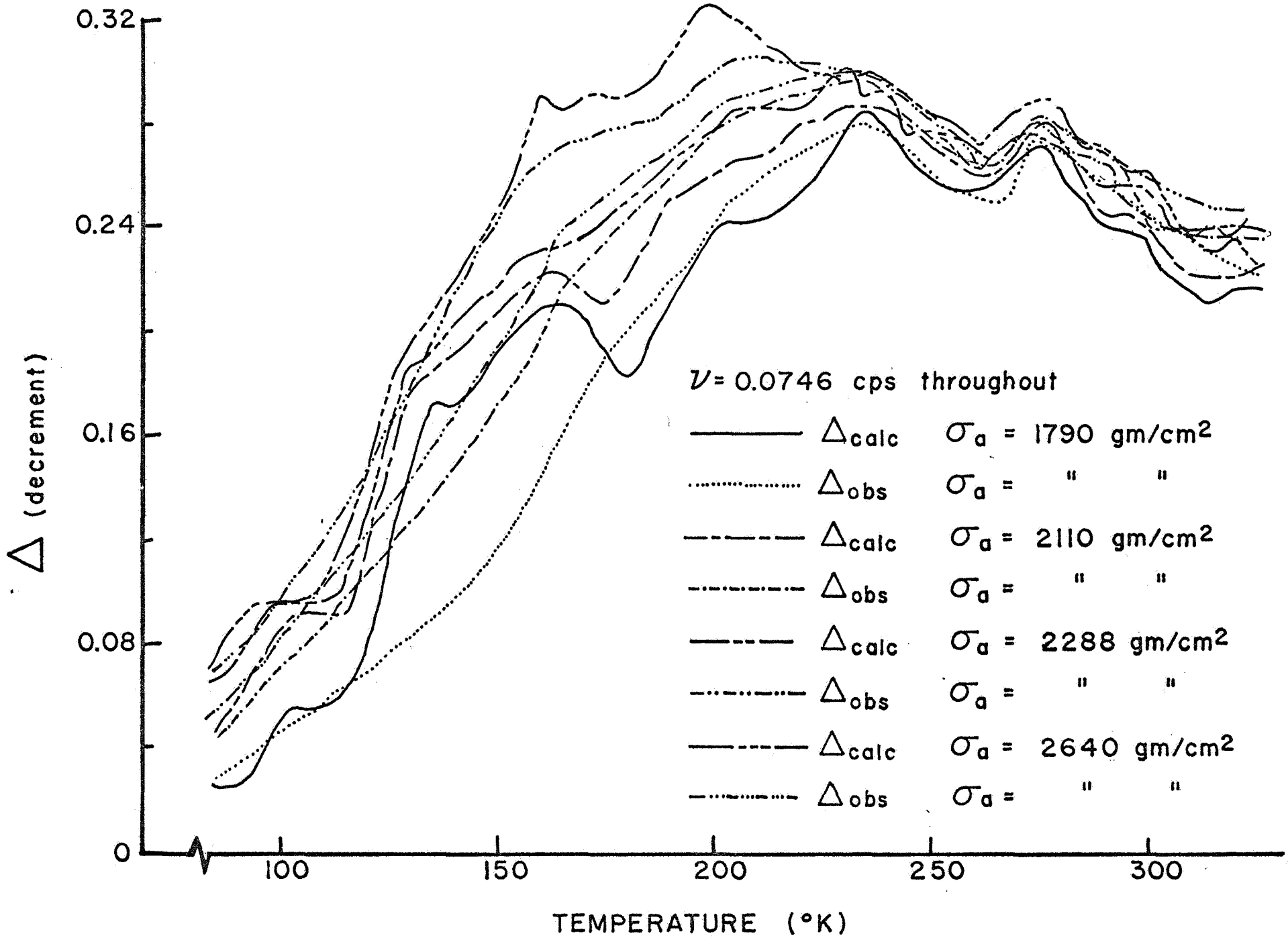

FIGURE 4: Δ_{obs} and Δ_{calc} versus T at four stresses and one frequency for crystal MS-3.

FIGURE 5: Δ_{obs} and Δ_{calc} versus T at one stress (1930 gm/cm^2) and frequency for crystal MS-3. The twenty eight processes contributing to Δ_{calc} are shown.

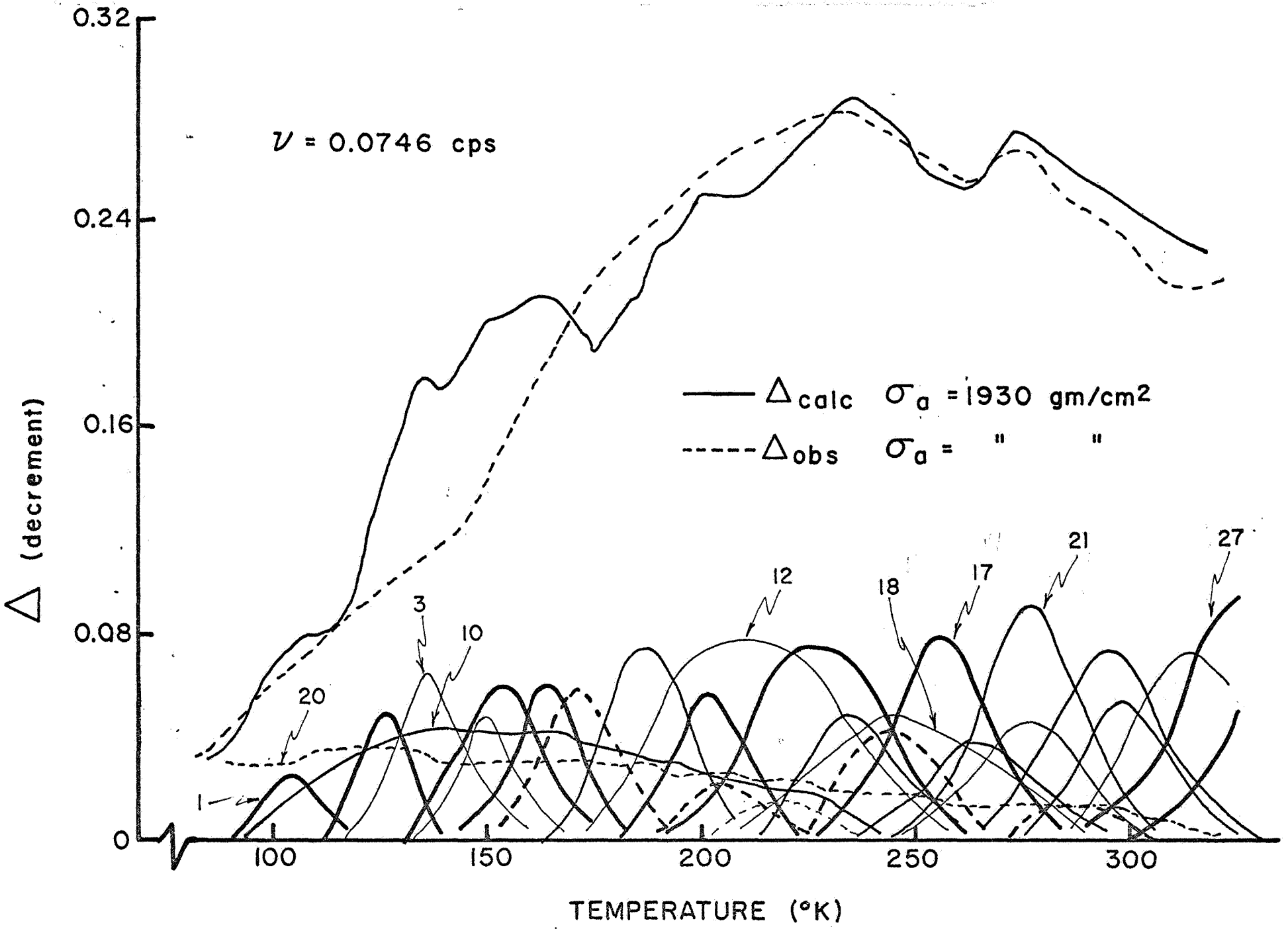

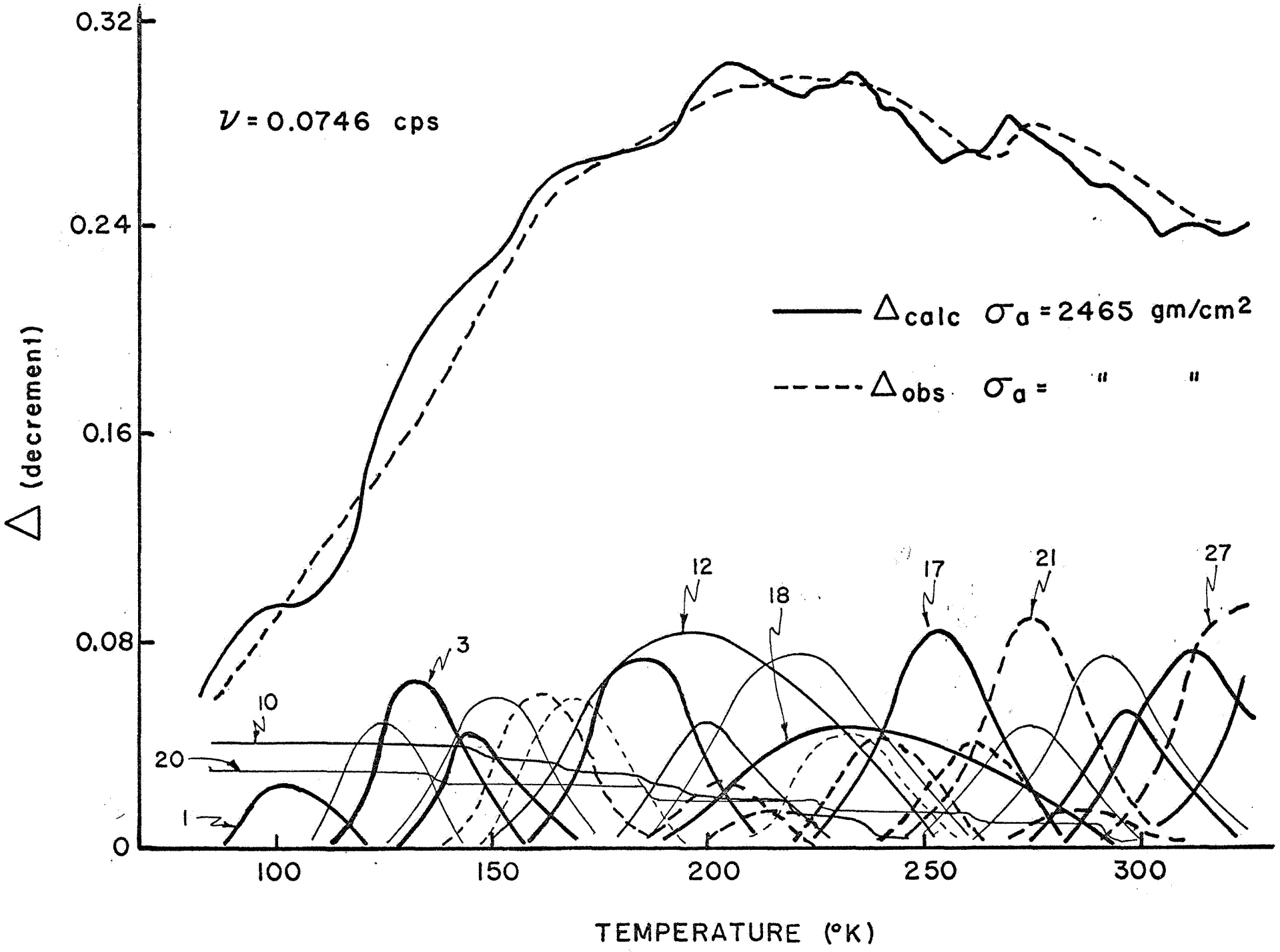

FIGURE 6: Δ_{obs} and Δ_{calc} versus T at one stress (2465 gm/cm^2) and frequency for crystal MS-3. The twenty-eight processes contributing to Δ_{calc} are shown.

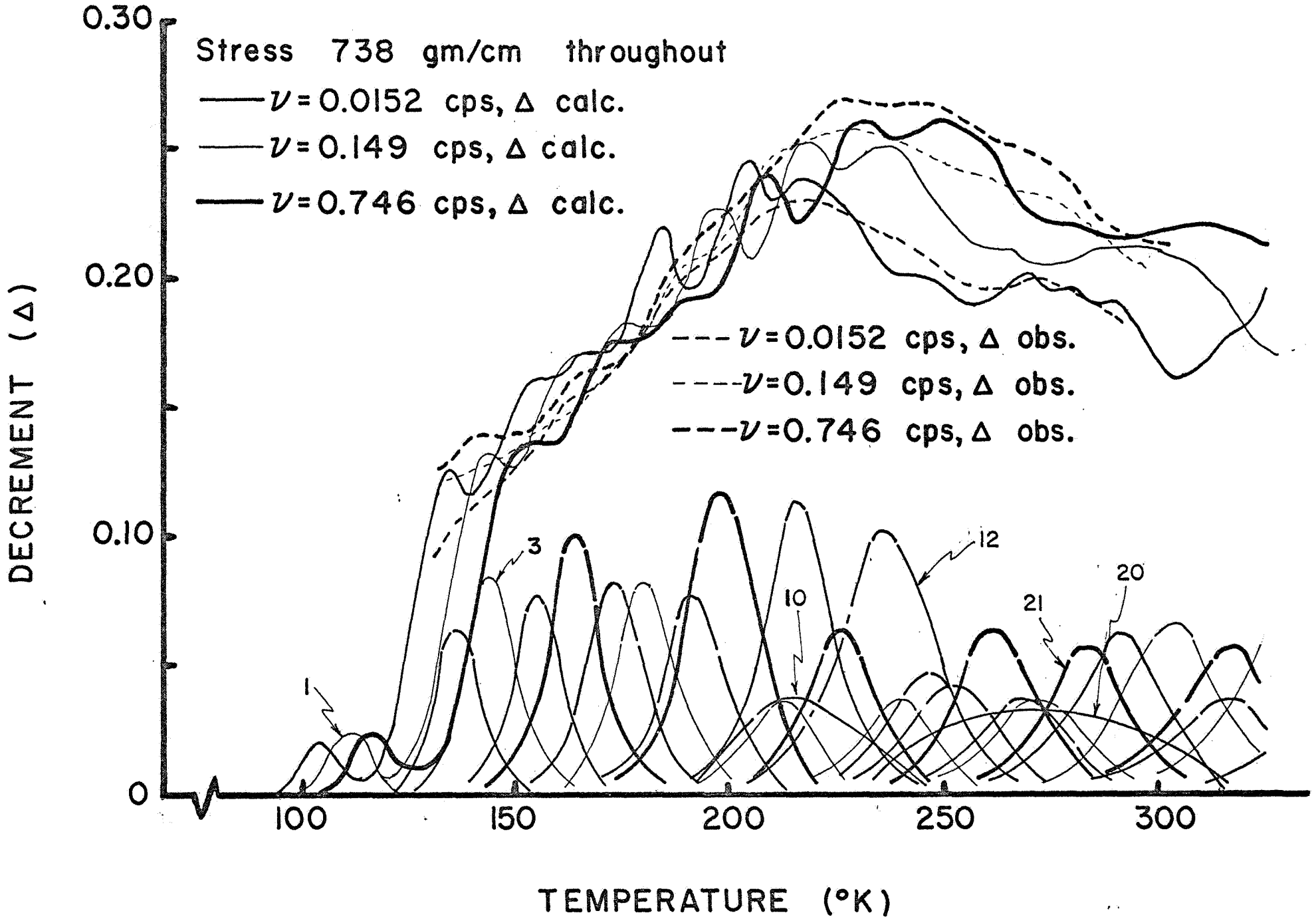

FIGURE 7: Δ_{obs} and Δ_{calc} versus T at 738 gm/cm^2 and three frequencies for crystal MS-6. The twenty-nine processes contributing to Δ_{calc} at the intermediate frequency are shown.

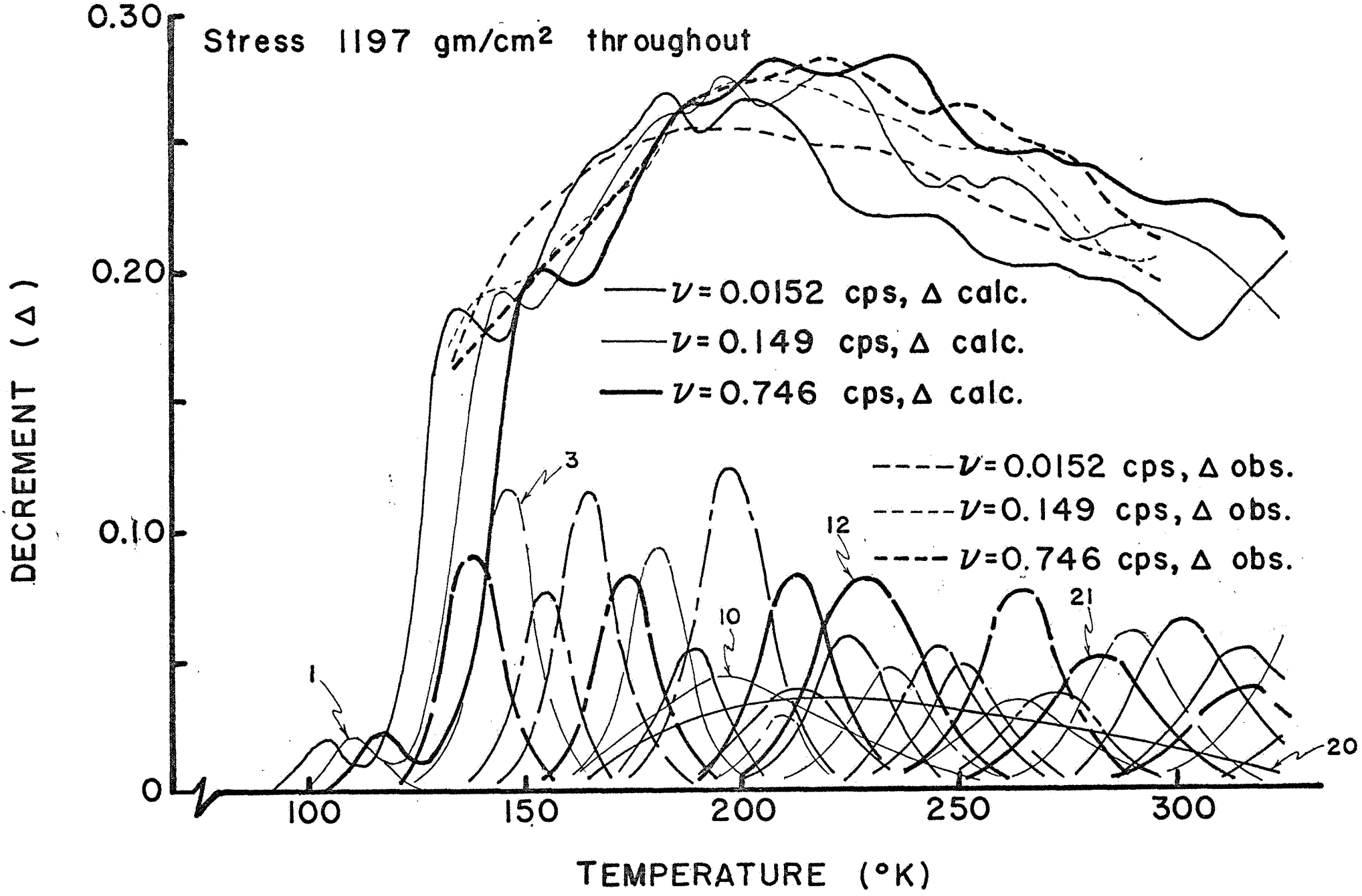

FIGURE 8: Δ_{obs} versus Δ_{calc} versus T at 1197 gm/cm^2 and three frequencies for crystal MS-6. The twenty-nine processes contributing to Δ_{calc} at the intermediate frequency are shown.

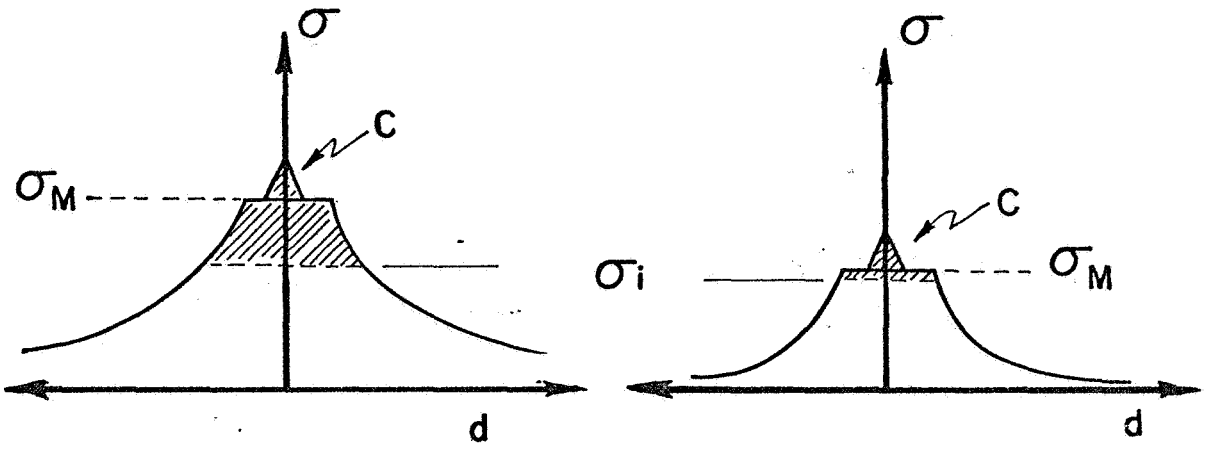

(a)

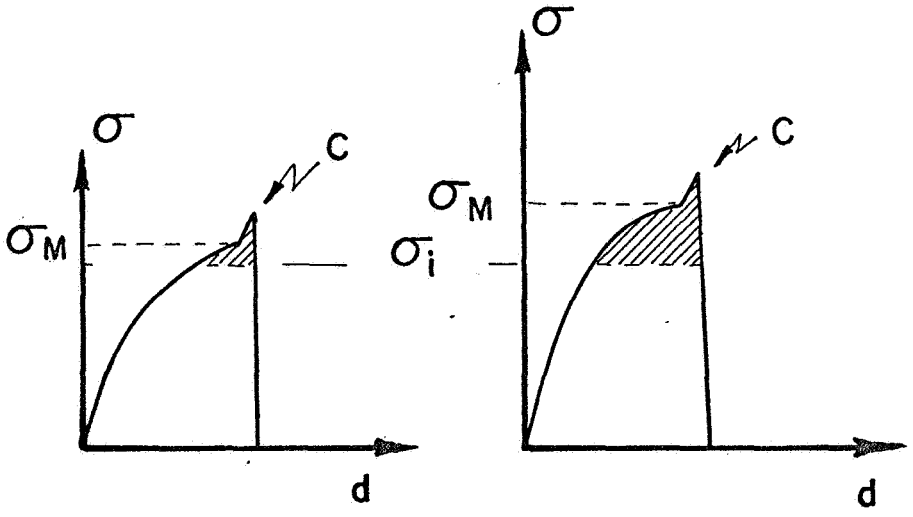

(b)

FIGURE 9: Schematic illustration of stress (σ) - displacement (d) curves for a mobile dislocation interacting with a forest dislocation.

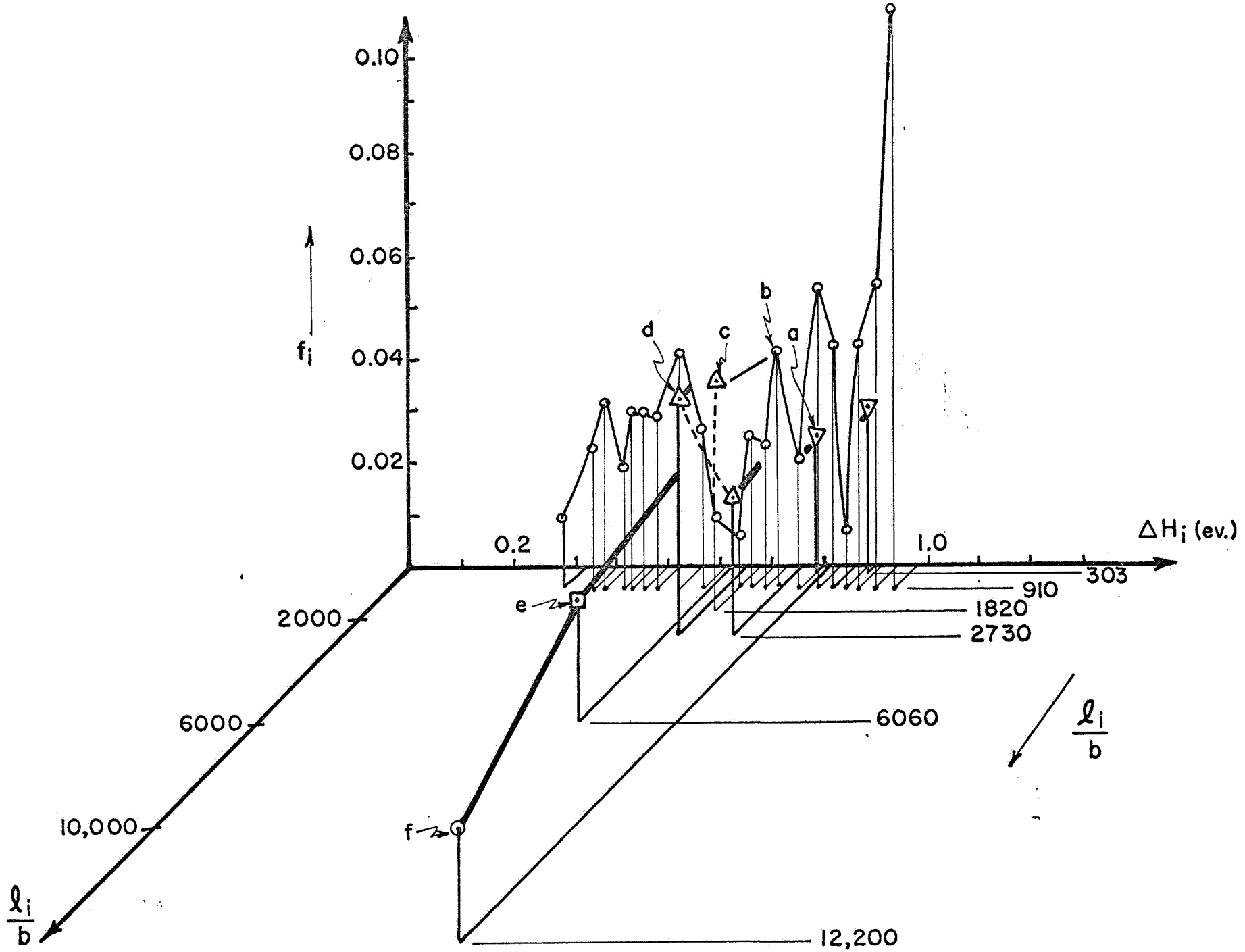

FIGURE 10: Plot of f_i versus ℓ_i/b and ΔH_i for the twenty-eight calculated processes described in Table II.